HHS Public Access

Author manuscript

Pain. Author manuscript; available in PMC 2022 February 01.

Published in final edited form as:

Pain. 2021 February 01; 162(2): 446–458. doi:10.1097/j.pain.0000000000002033.

Sex-dependent role of microglia in disulfide HMGB1-mediated mechanical hypersensitivity

Nilesh M Agalave[1,3,*], **Resti Rudjito**[1,*], **Alex Bersellini Farinotti**[1], **Payam Emami Khoonsari**[1,2], **Katalin Sandor**[1], **Yuki Nomura**[1], **Thomas A Szabo-Pardi**[3], **Carlos Morado Urbina**[1], **Vinko Palada**[1], **Theodore J Price**[4], **Helena E Harris**[5], **Michael D Burton**[3,*], **Kim Kultima**[1,2,*], **Camilla I Svensson**[1,*,**]

[1]Department of Physiology and Pharmacology, Center for Molecular Medicine, Karolinska Institutet, Stockholm 171 76, Sweden.

[2]Department of Medical Sciences, Clinical Chemistry, Uppsala University, Uppsala 751 85, Sweden.

[3]Neuroimmunology and Behavior Group, School of Behavioral and Brain Sciences, University of Texas at Dallas, Richardson, TX 75080, USA.

[4]Pain Neurobiology Research Group, School of Behavioral and Brain Sciences, University of Texas at Dallas, Richardson, TX 75080, USA.

[5]Department of Medicine, Center for Molecular Medicine, Karolinska Institutet, Stockholm 171 76, Sweden.

Abstract

High mobility group box 1 protein (HMGB1) is increasingly regarded as an important player in the spinal regulation of chronic pain. While it has been reported that HMGB1 induces spinal glial activation in a Toll-like receptor (TLR)4-dependent fashion, the aspect of sexual dimorphisms has not been thoroughly addressed. Here, we examined whether the action of TLR4-activating, partially reduced disulfide HMGB1 on microglia induces nociceptive behaviors in a sex-dependent manner. We found disulfide HMGB1 to equally increase microglial Iba-1 immunoreactivity in lumbar spinal dorsal horn in male and female mice, but evoke higher cytokine and chemokine expression in primary microglial culture derived from males compared to females. Interestingly, TLR4 ablation in myeloid-derived cells, which include microglia, only protected male mice from developing HMGB1-induced mechanical hypersensitivity. Spinal administration of the glial

**Corresponding author: Prof. Camilla I Svensson: Center for Molecular Medicine L8:03, Visionsgatan 18, 171 76 Stockholm, Sweden., Phone: +46 8 524 87948; Fax: +46 8 310622; camilla.svensson@ki.se.

Author contributions: N.M. Agalave, R. Rudjito, K Kultima and C.I. Svensson designed the study and discussed the outcome of experiments. N.M. Agalave performed cell culture and behavioral experiments. R. Rudjito performed western blot and behavioral experiments. T. Szabo-Pardi performed behavioral experiment. A. Bersellini Farinotti optimized protocols for immunohistochemistry and analyses were performed by A. Bersellini Farinotti, K. Sandor and C. Morado Urbina. N.M. Agalave and K. Sandor performed intrathecal injections. Y. Nomura generated primary microglial cell culture. P.E. Khoonsari performed LC-MS/MS and analyses were performed by P.E. Khoonsari, V. Palada and K. Kultima. T.J. Price and M.D. Burton provided PAR2$^{-/-}$ and LysM-TLR4$^{fl/fl}$ mice. H.E. Harris provided HMGB1 reagents. N.M. Agalave wrote the initial manuscript. All co-authors provided critical feedbacks and R. Rudjito, K. Kultima and C.I. Svensson revised the manuscript.

*These authors contributed equally to this manuscript

Conflict of interest

The authors declare no competing financial interests.

inhibitor, minocycline, with disulfide HMGB1 also prevented pain-like behavior in male mice. To further explore sex difference, we examined the global spinal protein expression using liquid chromatography-mass spectrometry (LC-MS/MS) and found several antinociceptive and anti-inflammatory proteins to be upregulated in only male mice subjected to minocycline. One of the proteins elevated, alpha-1-antitrypsin, partially protected males but not females from developing HMGB1-induced pain. Targeting downstream proteins of alpha-1-antitrypsin failed to produce robust sex differences in pain-like behavior, suggesting that several proteins identified by LC-MS/MS are required to modulate the effects. Taken together, the current study highlights the importance of mapping sex dimorphisms in pain mechanisms and point to processes potentially involved in the spinal antinociceptive effect of microglial inhibition in male mice.

Keywords

HMGB1; microglia; sex dimorphism; spinal; LC-MS/MS; minocycline; pain

Introduction

Although originally described as a nuclear protein, high mobility group box 1 protein (HMGB1) has reemerged as a pathogenic mediator of various diseases and injured states, including chronic pain [4]. HMGB1 can be passively or actively released by various cells, of which immune cells, glial cells and neurons have been suggested as sources of nociception-modulating HMGB1 [4; 23; 49]. Conversely, endogenous HMGB1 induces production of inflammatory mediators that consequently stimulate glial cells and neurons, and thus nociception [5; 52]. The redox state of extracellular HMGB1 serves as a key regulator of receptor binding and immune responses. Reduction of cysteines at positions C23, C45 and C106 generates all-thiol HMGB1, which binds to receptor for advanced glycation end-products (RAGE) and evokes chemotactic activity via interactions with the CXCL12/CXCR4 axis [59]. In contrast, disulfide HMGB1 is formed due to disulfide linkage between C23 and C45 and serves as a cytokine-inducing Toll-like receptor (TLR)4 ligand [64]. Although initial studies on HMGB1 isoforms and receptor interactions have been exclusively done in male subjects, accumulating data show that similar interactions also occur in females [1; 3; 5].

Spinal delivery of recombinant HMGB1 lowers the response threshold to calibrated touch and pressure stimuli in naïve rats and mice [3; 45]. This action of HMGB1 has been coupled to TLR4 activation as only disulfide HMGB1 induces mechanical hypersensitivity following intrathecal (i.t.) injection, which is prevented in TLR4-deficient mice. In addition, spinal disulfide HMGB1 upregulates a myriad of factors frequently associated with glial activation in a TLR4-dependent fashion [3].

Microglia are tissue-resident immune cells of the central nervous system (CNS), highlighted in recent years as having important roles in pain. In particular, there is a growing body of evidence that argues for a sexually dimorphic microglial involvement in chronic pain. Conventionally, most pain studies have been carried out in male rodents, however accumulating evidence points to sex differences in pain mechanisms. Of note, it has been

suggested that microglia are only required for pain processing in males, while females utilize the adaptive immune system. This proposition is based on observations that i.t. injection of microglial inhibitors reversed mechanical allodynia in males, whereas T-cell involvement was reported in females [55]. Furthermore, others show that spinal TLR4 mediates inflammatory and neuropathic pain in male but not female mice [54]. These findings support a sex-dependent role of microglia in nociception as TLR4 is known to regulate microglial activation [35]. Nonetheless, the debate is still ongoing as others fail to report clear sex differences regarding the roles of both spinal microglia and TLR4 [17; 62]. We have previously found that i.t. disulfide HMGB1 induces pain-like behavior in both male and female mice, and attenuating the action of HMGB1 alleviates mechanical hypersensitivity in both sexes subjected to arthritis [3]. Thus, the purpose of this study was to examine if disulfide HMGB1 induces nociceptive signaling via microglial activation in a sex-dependent fashion. We also undertook a global protein approach to uncover potential targets that may underlie sex differences in male and female mice.

Materials and methods

Animals

All experiments were carried out in accordance with protocols approved by the local ethics committee for animal experiments in Sweden (Stockholm North Animal Ethics Board) and the USA (the Institutional Animal Care and Use Committee of the University of Texas at Dallas), and were in accordance with the International Association for the Study of Pain guidelines. C57BL/6 male and female mice (10–12 weeks, 20–25 g) were purchased from Charles River Laboratories (Freiberg, Germany) and Janvier Labs (Le Genest-Saint-Isle, France). Myeloid cell-specific TLR4 depleted male and female mice (LysM-TLR4$^{fl/fl}$) were generated as previously described [25]. In brief, TLR$^{fl/fl}$ mice were crossed with mice expressing Cre under LysM promoter. The resulting LysM-TLR4$^{fl/fl}$ and TLR4$^{fl/fl}$ (control mice) were backcrossed 8 generations to a C57BL/6 background at the University of Texas at Dallas. Wild-type (PAR2$^{+/+}$) and PAR2-deficient (PAR2$^{-/-}$) male and female mice were obtained from Jackson Laboratory (Bar Harbor, ME, USA) and bred at University of Texas at Dallas. Animals were housed in a pathogen free environment with five mice per cage with water and food *ad libitum* in animal facilities at Karolinska Institutet and University of Texas at Dallas in a pathogen free environment with standard temperature and 12 h light/dark cycle.

Drugs and drug delivery

Endotoxin free, disulfide HMGB1 was kindly provided by Dr. H. Yang (Feinstein Institute for Medical Research, NY, USA) or purchased from HMGBiotech (Milan, Italy). Minocycline (glial inhibitor), alpha-1-antitrypsin (A1AT, protease inhibitor) and sivelestat (neutrophil elastase inhibitor) were all purchased from Sigma-Aldrich (St Louis, MO, USA). Intrathecal (i.t.) delivery was performed in animals deeply anesthetized with 4% isoflurane and maintained on 2.5% isoflurane during the lumbar puncture procedure using a 30 G needle inserted into the space between L4-L5 vertebrae. Tail flick was noted as an indicator for a successful i.t injection. Animals were injected i.t with 1 μg disulfide HMGB1 or PBS as vehicle control. In pharmacological experiments, 1 μg disulfide HMGB1 was injected i.t.

either alone or in combination with 30 μg minocycline, 15 μg haptoglobin, 15 ng A1AT or 0.5 ng sivelestat. The following day the animals were given i.t. injection of either 30 μg minocycline, 30 ng A1AT, 1 ng sivelestat or vehicle (PBS). All reagents were injected in a total volume of 5 μL i.t.

Microglial culture

The murine microglial cell line N13 (CD1 strain) was kindly provided by Prof. Gunnar Schulte, Karolinska Institutet, Stockholm, Sweden. Cells were expanded in Dulbecco's modified Eagle's medium (DMEM, Gibco, Carlsbad, CA, USA) supplemented with 10% fetal bovine serum (FBS, Sigma-Aldrich, St. Louis, MO, USA), 2mM L-glutamine, 50 U/mL penicillin and 50 μg/mL streptomycin (Gibco) in a humidified incubator with 5% CO_2. Upon reaching 75–80% confluency, cells were dissociated with 0.25% trypsin-EDTA (Sigma-Aldrich) and seeded at 2.5×10^5 cells/well in 12-well plate in supplemented DMEM medium. Following overnight incubation to allow for cell attachment, cells were serum starved (0.5% FBS) for 24 h. Cells were stimulated with 1 μg/mL disulfide HMGB1 and collected 6 h later for qPCR analysis.

To generate primary microglial culture, male and female mice were deeply anesthetized with isoflurane and intracardially perfused with ice cold PBS containing 5mM EDTA to reduce the presence of blood mononuclear cells. Following decapitation, the skull cap was removed, and brain tissues were collected. Spinal column was cut at the level of the iliac crest and the spinal cord was extracted using hydroextrusion with 21-gauge needle and ice-cold PBS. Both tissues were then transferred into a 15 mL conical tube containing ice cold PBS until homogenization. To maximize cell yield, brain and spinal cords tissues from 2–3 mice were combined from the same sex for homogenization in each experiment. Microglia were then isolated and cultured using a modified version of previously described protocols [2; 53]. In brief, tissues were mechanically dissociated using sterile scalpels followed by enzymatic digestion with papain (2 mg/mL, Sigma-Aldrich) for 30 min at 37°C. The homogenate was centrifuged at 500*g* for 5 min at 4°C and microglial cells were isolated using Percoll density gradient. In brief, cell pellets were resuspended in microglial culture medium containing Dulbecco's modified Eagle's medium/nutrient mixture F-12 (DME/F12, Gibco, Carlsbad, CA, USA) supplemented with 10% fetal bovine serum (Sigma-Aldrich), 100 U/mL penicillin, 50 μg/mL streptomycin and 2 mM glutamine (Gibco), and centrifuged at 500*g* for 30 min at room temperature over a 37%/70% Percoll gradient (GE Healthcare, Princeton, NJ, USA). Microglial cells were then collected from the interface and the total cell number was determined using hemocytometer. Cells were seeded at 2.5×10^5 cells/well in a 48-well plate precoated with poly-D-lysine (Sigma-Aldrich) and incubated for 2 h at 37°C in microglial culture medium to allow for cell attachment. Subsequently, cells were serum starved (2% FBS) and maintained for 24 h in a humidified 37°C incubator with 5% CO_2. The next day, cells were stimulated with 1 μg/mL disulfide HMGB1 and collected 6 h later for qPCR analysis.

Behavioral tests

Animals were placed in wire mesh bottomed cages and allowed to habituate to the test environment before baseline measurement. Three baselines were measured on three different

days followed by randomization of the animals into treatment groups. Mechanical hypersensitivity was assessed using calibrated von Frey filaments (Marstock, Marburg, Germany and Stoelting, Wood Dale, IL, USA) applied on the plantar surface of the hind paws using the up-down method [12]. The filament was applied for 2–3 seconds or until a brisk withdrawal was observed. Paw withdrawal thresholds were recorded in grams and calculated as percentage change of the respective mean baseline values. The effect of i.t. disulfide HMGB1 on mechanical hypersensitivity in wild-type and genetically modified mice (LysM-TLR4$^{fl/fl}$ and PAR$^{2-/-}$) was assessed 6 h and then once a day until day 5 post-injection. In pharmacological experiments with minocycline, haptoglobin, alpha-1-antitrypsin and sivelestat, mechanical hypersensitivity was evaluated 3, 6 and 24 h following the first i.t. injection when HMGB1 and one of the inhibitors were co-administered, and then 3 and 6 h following the second i.t. injection when the inhibitors were injected alone. All behavioral experiments were performed during day cycle in a blinded fashion.

Quantitative real-time PCR

Cells were washed with pre-chilled PBS and homogenized in TRIzol reagent (Invitrogen, Carlsbad, CA, USA). mRNA was extracted according to manufacturer's protocol followed by cDNA synthesis using MultiScribe™ Reverse Transcriptase (Invitrogen) and qPCR using StepOne™ Real-Time PCR Systems (Applied Biosystems, Foster City, CA, USA). Predeveloped probes for *Tnf* (Mm00443258_m1), *Il1b* (Mm00434228_m1), *Il6* (Mm00446190_m1), *Ccl2* (Mm00441242_m1) and *Hprt1* (Mm01545399_m1) (all from Applied Biosystems) were used for mRNA analyses. Threshold cycle values for each sample were used to calculate the number of cell equivalents using the standard curve method [11]. The data were normalized to the housekeeping *Hprt1* mRNA levels and expressed as percentage change of the control group.

Immunohistochemistry

Animals were deeply anesthetized with isoflurane and intracardially perfused with PBS followed by 4% formaldehyde at 24 h post i.t. injection of either 1 μg disulfide HMGB1 or PBS. Lumbar spinal cords (L3-L5) were then dissected followed by post-fixation in 4% formaldehyde for 20 h and cryoprotection in 20% sucrose solution for 24 h. Spinal cords were embedded in OCT (Histolab, Gothenburg, Sweden), frozen with liquid CO_2 and cut at 20 μM using CryoStar NX70 cryostat (ThermoFisher Scientific, Bremen, Germany). Tissue sections were incubated with rabbit anti-Iba1 antibody (1:2000, cat no. 019–19741, Wako, Richmond, VA, USA,) and horseradish peroxidase (HRP)-conjugated anti-rabbit secondary antibody (1:200, cat no. P0448, Dako, Glostrup, Denmark). Immunoreactivity was visualized with TSA Plus kit (Perkin Elmer, Waltham, MA, USA) according to manufacturer's protocol. Stained sections were mounted with Prolong Gold antifade mounting medium (ThermoFisher Scientific) and examined by LSM710 confocal microscope (Carl Zeiss, Jena, Germany). The immunoreactivity (IR) intensity of the left and right dorsal horn was measured after manually outlining lamina I-VI and subtracting background signals using ImageJ (NIH, Bethesda, MD, USA). Three L4 sections separated at least 50 μM from each other were analyzed per animal and the IR intensity averaged. An increase in IR intensity was considered as a sign of increased microglial reactivity [47]. The

analyses were performed by two independent investigators that were blinded to the treatment groups

Protein extraction

Mice were euthanized 6 h post-injection and lumbar spinal cords were collected by hydroextrusion, snap frozen and stored at −80°C. For protein extraction, samples were disrupted in a lysis buffer containing PBS, 1% SDS and a cocktail of protease inhibitors (Roche, Mannheim, Germany) and subjected to repeated freeze thawing and sonication for 10–15 s (0.3s on 0.7s pulse) using a tip sonicator. Protein concentration was estimated using standard Pierce™ BCA assay kit (ThermoFisher Scientific) according to manufacturer's protocol. For LC-MS/MS, protein samples were further alkylated and reduced by the addition of dithiothreitol and iodoacetamide (Sigma-Aldrich), followed by overnight acetone precipitation. Protein pellets were then enzymatically digested in endoproteases Lys-C and trypsin (Sigma-Aldrich) overnight and stored at −20°C.

Liquid chromatography–mass spectrometry (LC-MS/MS)

The peptide samples were labeled using TMT6 plex isobaric label reagent set (ThermoFisher Scientific) according to manufacturer's protocol. One mouse from each treatment group (four in total) was assigned to a TMT6 plex, including two pools of all samples for each TMT6 plex. The TMT-labeled peptide samples were pre-fractionated using high pH reverse-phase liquid chromatography (12 fractions that were pooled into five fractions for each TMT6 plex). The fractions were evaporated, reconstituted in 20 μL 0.1% formic acid and 4 μL were analyzed by high-resolution nano LC-MS/MS using an Q-Exactive mass spectrometer (Thermo Fisher Scientific) coupled to high-performance nanoLC systems (Dionex Ultimate-3000, Thermo Fisher Scientific) set up in a trap (Acclaim PepMap 2 cm, 3 μm C18) and elute (50 cm EasySpray™ PepMap™ RSLC C-18) configuration (both Thermo Fisher Scientific). The LC gradient buffers consisted of A (3% acetonitrile, 0.1% formic acid in LC-MS grade water) and B (96% acetonitrile, 0.1% formic acid in LC-MS grade water) components. The buffer B gradually increased from 3 to 37% in 150 min, to 47 % in the next 20 min and 99% in the next 9 min. The column was equilibrated for an additional 11 min before the next sample was injected. Peptides were eluted at a flow rate of 250 nL/min and equilibration at 400 nL/min. MS spectra were acquired in a data-dependent acquisition (top 12) in full MS mode at 70,000 resolution (scan range of 300 to 1600 m/z) and further fragmented in MS/MS mode performed by collision-induced dissociation (arbitrary unit of 33) at 35,000 resolution (scan range of 100 to 2000 m/z).

Protein identification

The raw MS data was converted to an open source format (mzML) by "msconvert" from ProteoWizard [30] and processed using OpenMS [48] through the following workflow: for identification the UniProt/Swiss-Pro mus musculus database (release 2017_07) combined with a decoy database (the sequences were reversed) was used in MS-GF+ search engine [31] (precursor mass tolerance: 10 ppm; enzyme: trypsin; min precursor_charge: 2; max precursor charge:4; fixed modifications: Carbamidomethyl (C), TMT6plex (N-term and K); variable modifications: Oxidation (M), Deamidated (N and Q), Acetyl (N-term). The result was imported into Percolator [27] and peptides matches with a q-value<0.05 were used in

Fido [50] to score proteins based on peptide-spectrum matches. The proteins with q-values<0.05 were selected for subsequent analysis. For quantification, “IsobaricAnalyzer” were used to find and quantify the peptides using TMT6Plex correction matrix. The resulting features and peptides from the identification stages were mapped together using “IDMapper” (m/z tolerance: 5 ppm; RT tolerance: 2 s). The corresponding peptides and features across the samples were matched using the “FeatureLinkerUnlabeledQT” (m/z tolerance: 5; RT tolerance: 20 s). Peptide abundances were aggregated to protein abundances using “ProteinQuantifier”, in which the intensity of the peptides (protein q-values<0.05) were summed. The result was imported to the statistical software environment R (R Core Team (2013). R: A language and environment for statistical computing. R Foundation for statistical Computing, Vienna, Austria. http://www.R-project.org/) and $\log_2$ transformed. The protein abundance in each sample was subtracted from the global pool within TMT set. The proteins were limited to the ones that were identified with at least two peptides and quantified in both treatment groups (irrespective of gender) with less than 50% missing values. Finally, the protein abundances were normalized using an in-house version of cyclic loess normalization [7] (https://github.com/PayamEmami/limma).

Western Blot

Proteins were separated using gel electrophoresis and transferred to nitrocellulose membrane (ThermoFisher Scientific). Non-specific binding sites were blocked with 5% non-fat milk in Tris based-buffer (50 mmol/L Tris-HCl and 6 mmol/L NaCl with 0.1% Tween 20). Afterwards, the membranes were incubated overnight with primary antibodies followed by HRP-conjugated secondary antibodies. Primary antibodies used were goat anti-haptoglobin (1:1000, cat no. GHPT-90A-Z, ICL, Portland, OR, USA), goat anti-alpha-1-antitrypsin (1:2000, cat no. AF2979, R&D Systems, Minneapolis, MN, USA), sheep anti-ELA2 (1:1000, cat no. AF4517, R&D Systems), rabbit anti-PAR2 (1:250, cat no. 180953, Abcam, Cambridge, UK) and mouse anti-GAPDH (1:10,000, cat no. ab8245, Abcam, Cambridge, UK), while secondary antibodies used were anti-goat (1:7500, cat no. ab6685, Abcam), anti-sheep (1:5000, cat no. 12–342, Sigma-Aldrich), anti-rabbit (1:500, cat no. 7074, Cell Signaling, Danvers, MA, USA) and anti-mouse (1:5000, cat no. 7076, Cell Signaling). Chemiluminescent reagent was used to visualize immunopositive bands (ThermoFisher Scientific) and signal intensity was measured using Quantity One software (Bio-Rad, Hercules, CA, USA). Immunopositive bands were normalized to the bands of GAPDH, and results are presented as percentage change to the respective control group.

Statistical analyses

Differences between two groups were assessed by unpaired two-tailed student’s *t*-test, whereas differences between groups split into two independent variables were analyzed by two-way ANOVA followed by Tukey post hoc test using GraphPad Prism (San Diego, CA, USA). P-values less than 0.05 were considered statistically significant. For LC-MS/MS data, the data was imported to R, transformed into $\log_2$ scale and multiple linear models were fitted (using a classical 2 × 2 factorial design) through the proteins and moderated statistics was calculated (f-statistics for the global tests, t-statistics for individual contrasts and corresponding p-values and fold changes) using the “limma” package [46] in R. The following six contrasts were included in the model: “Global sex difference: ((MalesH +

MalesHM) - (FemalesH + FemalesHM))", "Sex difference: (MalesH-FemaleH)", "Global treatment effect: ((MalesHM + FemalesHM) - (MalesH + FemalesH))", "Treatment effect in males: (MalesHM- MalesH)", "Treatment effect in females: (FemalesHM- FemalesH)", "Difference in sex after treatment: (MalesHM-FemalesHM)" and "The interaction effect: (MalesHM-MalesH) – (FemalesHM-FemalesH)". "H" denotes only HMGB1 injection and "HM" denotes HMGB1 injection followed by minocycline. The moderated statistics were converted to regular statistics using an in-house function (https://github.com/PayamEmami/limma). To correct for multiple testing the resulting p-values (ANOVA p-values) were transformed to q-values [28] using "q-value" package in R. For significant proteins (q-value<0.05), a Venn diagram was constructed showing the result of "Global sex difference", "Global treatment effect" and "The interaction effect", using a p-value<0.05 for each individual contrast. To ease interpretation, bar plots using FemalesH as baseline ("MalesH-FemalesH", "MalesHM-FemalesH" and "FemalesHM-Females H") were constructed.

Results

Intrathecal injection of disulfide HMGB1 induces morphological changes related to microglial reactivity in lumbar spinal cords of male and female mice

In an earlier study, we have demonstrated that i.t. disulfide HMGB1 increases mRNA levels of the microglial marker *Cd11b* in the spinal cord. However, that study was only performed in male mice [3]. Therefore, to examine whether male and female mice exhibit a similar pattern of microglial reactivity, we stained lumbar spinal cord sections with the microglial marker ionized calcium binding adaptor molecule 1 (Iba1). A morphological change in the form of larger cell bodies and more ramified processes was observed for the majority of Iba1-stained cells in the dorsal horn 24 h after i.t. disulfide HMGB1 in both sexes (Fig. 1 A, B). We observed significantly higher intensity of the Iba1 signal in both male (140.9 ± 13.0 vs. 100.0 ± 7.2 %, n=6, p=0.02) and female (123.2 ± 1.9 vs. 100.0 ± 7.6 %, n=5, p= 0.02) mice subjected to disulfide HMGB1 injection compared to the respective saline control groups (Fig. 1 C, D).

Disulfide HMGB1 stimulation induces higher proinflammatory mediators in cultured microglia derived from male compared to female mice

We have previously shown that i.t. disulfide HMGB1 drives cytokine and chemokine expression frequently associated with glial activation in the spinal cord such as *Tnf*, *Ilb*, *Il6* and *Ccl2* [3]. In order to examine whether HMGB1 has a direct action on microglia we first used the microglial cell line N13 and found that disulfide HMGB1 evoked increased gene expression of *Tnf*, *Ilb*, *Il6* and *Ccl2* (Fig. S1A–D). However, as the sex of the mouse used for establishment of the N13 cell line is not readily available, we utilized primary microglial culture generated from brain and spinal cord tissues to examine if the response to disulfide HMGB1 differs between microglia from males versus females. Cultured microglia were stimulated with disulfide HMGB1 for 6 h followed by mRNA isolation and measurement of cytokine and chemokine expression by qPCR. Exposure to disulfide HMGB1 for 6 h led to an increase of *Tnf*, *Ccl2* and *Il1b* mRNA levels compared to unstimulated cells in male-derived but not female-derived microglia, although there was a trend towards an increase of *Il1b* mRNA levels in female microglia following disulfide HMGB1 stimulation albeit not

significant (Fig. 2A–C). In contrast, disulfide HMGB1 induced *Il6* expression to similar levels in both sexes (Fig. 2D). As 2–3 mice of each sex were pooled to generate primary cultures in this experiment, n represents experimental replicates. The experiment was repeated twice with similar results.

Inhibition of spinal microglial function attenuates disulfide HMGB1-induced mechanical hypersensitivity in male but not female mice

Spinal injection of disulfide HMGB1 evokes mechanical hypersensitivity in both male and female mice [3], however whether the underlying mechanism is regulated by microglia in a sex-dependent fashion is not known yet. In order to investigate this, we undertook two different approaches to inhibit microglial function, and therefore disrupt their interaction with disulfide HMGB1 in both male and female mice. The first approach was using conditional knockout mice that lack TLR4 in myeloid-derived cells, which includes microglia (LysM-TLR4$^{fl/fl}$) [25]. Spinal delivery of disulfide HMGB1 in LysM-TLR4$^{fl/fl}$ mice did not elicit mechanical hypersensitivity in males (Fig. 3A), whereas females displayed lower mechanical thresholds than vehicle injected mice and were of similar levels to the injected control TLR4$^{fl/fl}$ mice (Fig. 3B). The second approach was using minocycline, a drug that is frequently used as a microglial inhibitor. Disulfide HMGB1 was injected i.t. either alone or in combination with minocycline, followed by a second i.t. injection of either vehicle (PBS) or minocycline 24 h later. Co-injection with minocycline prevented disulfide HMGB1-induced mechanical hypersensitivity in male but not female mice 6 h postinjection on the first day. A second minocycline injection the following day significantly reversed pain-like behavior only in male mice previously injected with disulfide HMGB1 (Fig. 3C, D).

Global protein expression profile of the lumbar spinal cords displays sex dimorphism in response to minocycline treatment

We used LC-MS/MS to identify possible targets that underlie sex differences in the spinal cords between male and female mice subjected to disulfide HMGB1 alone, or in combination with minocycline. The first treatment group is referred to as “vehicle” group, and the latter as “minocycline” group. Lumbar spinal cords were collected 6 h after the second i.t. injection and subsequently processed for LC-MS/MS. In total, 2947 proteins were identified and relatively quantified. Using a 2×2 factorial design, we found 54 proteins to be differentially expressed in male and female mice in both vehicle and minocycline groups ($q<0.05$). Out of these, 36 proteins were differentially expressed in both sexes in the vehicle group. In males, differences in expression were observed in 44 proteins between vehicle and minocycline group, which is in contrast to only 8 proteins being affected in females (Table S1). Proteins that showed significant interaction between sexes and minocycline were narrowed down to 12 proteins (Fig. 4). A total of 8 out of 12 proteins were upregulated in male minocycline group as compared to vehicle group, while we observed minimal or opposite effects on female mice (Fig. 5A–H). The protein with the largest effect size between male and female vehicle groups was alpha-1-antitrypsin 1–5 (A1AT5). Interestingly, A1AT5 also showed the largest effect size in male mice in response to minocycline treatment (Fig 5A). Beside A1AT5, other isoforms of alpha-1-antitrypsin, A1AT4 and A1AT2 were upregulated in male minocycline group (Fig. 5B, C) alongside with

serine protease inhibitor A3K (SPA3K), SPA3N, haptoglobin (HPT), hemopexin (HEMO), and vitamin D binding protein (VDBP) (Fig. 5D–H). None of these proteins were significantly altered in response to the minocycline treatment in female mice (Fig. 5A–H).

Alpha-1-antitrypsin but not its downstream target neutrophil elastase elicits partial antinociceptive properties in a sex-dependent manner

By western blot, we validated the changes in haptoglobin expression observed in LC/MS-MS in which haptoglobin was upregulated in male but down-regulated in female mice in the minocycline group (Fig. S2A, B). Recent work shows that haptoglobin binds to HMGB1 and counter-regulates the pro-inflammatory properties of HMGB1 by skewing macrophage polarization towards an anti-inflammatory phenotype [65]. Interestingly, this study was only done in male mice and therefore it is not known whether a similar action of haptoglobin on HMGB1 occurs in female mice. Given the fact that haptoglobin is elevated in male but reduced in female minocycline group suggests that haptoglobin may serve as a protective mechanism for HMGB1-induced hypersensitivity in male mice. Therefore, we examined whether haptoglobin may be responsible for the antinociceptive effect of minocycline in male mice. Our findings, however, show that co-injection of haptoglobin (15 μg) with disulfide HMGB1 (1 μg) did not prevent HMGB1-induced mechanical hypersensitivity in both male and female mice (Fig. S2C, D).

The next target protein that we examined was alpha-1-antitrypsin and neutrophil elastase (Fig. 6A). Unlike humans, where only one essential gene is known, alpha-1-antitrypsin in mice occurs in multiple isoforms encoded by up to 5 polymorphic genes depending on the substrains [9]. The strain that was used for this study, C57BL/6, harbors 5 paralogs, in which 3 out of 5 paralogs were upregulated in male mice of the minocycline group. We confirmed that alpha-1-antitrypsin expression was elevated in male but not female mice in response to minocycline treatment (male: 576 ± 84 vs. 100 ± 15 %, n=6, p=0.0002, female: 72 ± 12 vs. 100 ± 13 %, n=6, p=0.1) (Fig. 6B) by western blot. Of note, the antibody used to detect alpha-1-antitrypsin does not differentiate between paralogs. Alpha-1-antitrypsin is characterized as a potent inhibitor of serine proteases, in particular neutrophil elastase [9], which has recently been implicated in both inflammatory and neuropathic pain [43; 44; 60]. To examine whether elastase was a possible downstream target of the pronociceptive cascade inhibited by alpha-1-antitrypsin in male mice, we analyzed neutrophil elastase protein expression using western blot. Indeed, we found a reduction of elastase (ELA2) protein expression in male mice treated with minocycline compared to vehicle (70 ± 4 vs. 100 ± 9 %, n=6, p=0.02) (Fig. 6C). By contrast, female mice showed equivalent levels of ELA2 expression in both minocycline and vehicle groups (99 ± 10 vs. 100 ± 26 %, n=6, p=0.9) (Fig. 6C).

Next, we investigated whether spinal injection of alpha-1-antitrypsin with disulfide HMGB1 would provide protection in mice from developing mechanical hypersensitivity. Co-administration of alpha-1-antitrypsin (15 ng/mouse) and disulfide HMGB1 (1 μg) into the spinal cord did not prevent HMGB1-induced pain-like behavior in either male or female mice (Fig. 6D, E). The following day, a higher dose of only alpha-1-antitrypsin (30 ng/mouse) was i.t. injected. A partial reversal in mechanical hypersensitivity was observed 3 h

after i.t. injection of alpha-1-antitrypsin in male, but not female mice (Fig. 6D, E). Interestingly, i.t. injection of the neutrophil elastase inhibitor sivelestat [29] (0.5 ng) together with HMGB1 (1 μg) did not prevent or reverse disulfide HMGB1-induced pain-like behavior in either sex of mice (Fig. 6D, E), even though the dose of sivelestat was doubled on the second day similar to the study with alpha-1-antitrypsin.

PAR2 depletion partially protects both male and female mice from disulfide HMGB1-induced pain

Neutrophil elastase induces neurogenic inflammation and pain via activation of proteinase-activated receptor 2 (PAR2) [44; 67] expressed by nociceptors [22]. We hypothesized that alpha-1-antitrypsin directly inhibits neutrophil elastase, which subsequently blocks PAR2 activation. Counterintuitive to the results above, we found spinal PAR2 expression to be significantly decreased in both male and female mice receiving minocycline together with HMGB1 compared to vehicle i.t. (male: 80 ± 4 vs. 100 ± 7 %, n=5, p=0.03, female: 69 ± 6 vs. 100 ± 5 %, n=6, p=0.0003) (Fig. 7A, B). Of note, one data point in the male vehicle group was identified as an outlier using ROUT outlier test (Q = 1%) and therefore eliminated from the analysis. In accordance, both male and female whole-body PAR2 knockout ($PAR2^{-/-}$) mice were partially protected from development of disulfide HMGB1-induced mechanical hypersensitivity (Fig. 7C, D).

Discussion

The current study investigates if there is a sex-associated difference in TLR4-activating disulfide HMGB1-induced microglial activation and the mechanisms by which it drives pain-like behavior. Our results show that i.t. injection of disulfide HMGB1 increased microglial reactivity in both sexes based on morphology, but direct stimulation of cultured microglia with HMGB1 led to higher expression of cytokines and chemokines in males compared to females. Interestingly, attenuation of disulfide HMGB1-induced pain-like behavior was only achieved by the microglia inhibitor minocycline and TLR4 depletion in myeloid cells in male mice. We performed global proteomic analysis of the spinal cords, which revealed an increase in proteins associated with antinociceptive and anti-inflammatory effects in male receiving minocycline. Targeting these proteins alone, however, did not replicate the sex-dependent effects of minocycline on disulfide HMGB1-induced hypersensitivity. Together these results suggest that microglia regulate HMGB1-induced pain mechanisms in a sex-dependent manner.

We have previously reported that i.t. injection of disulfide HMGB1 induces pain-like behavior in male and female mice [3], however it is not known if disulfide HMGB1 promotes microglial activation similarly in both sexes. Following i.t. injection of disulfide HMGB1 spinal microglia in both male and female mice display the characteristic signs of activation such as enlarged cell bodies and increased Iba-1 immunoreactivity [38; 41; 58]. This is supportive of previous reports showing similar levels of microglial activation *in vivo* following nerve injury [54; 56]. Another feature of activated microglia is cellular production of pro-inflammatory mediators [10; 57]. In agreement with previous work showing that TLR4 activation by lipopolysaccharide (LPS) induces higher *Il1b* mRNA in male microglia

[37], we found that disulfide HMGB1 stimulation of cultured primary microglia induces more pronounced mRNA levels of *Il1b* and other cytokines in male-derived cells compared to the females. Thus, the degree of pro-inflammatory response of microglia to not only LPS but also HMGB1 stimulation is sex-dependent.

We found that blockade of microglial activation by disulfide HMGB1 resulted in prevention of pain-like behavior only in male mice. Our findings support earlier reports showing that spinal microglia and TLR4 are important for nociception in males [54; 55]. Given the fact that disulfide HMGB1 induced higher mRNA levels of inflammatory factors in male compared to female microglia supports the notion that there is a greater microglial involvement in male mice. HMGB1 can increase microglial activity through TLR2, TLR4 and RAGE receptor activation [18]. When it comes to the redox form of HMGB1, it is not known how long HMGB1 is retained in the disulfide form in the spinal cord after i.t. injection and if it differs between male and female mice. Thus, it is possible that the redox state of HMGB1 change over time in a fashion that enables HMGB1 to start to act on other receptors such as TLR2 [6], TLR5 [15], RAGE [32] or CD24/siglec10 [63]. If this modification is differentially regulated between male and female mice, it is possible that another receptor system mediates the effect of i.t. HMGB1 in female mice hence interfering with HMGB1-TLR4 interactions in females do not prevent pain-related behaviors.

To generate mice with TLR4-specific deletion in microglia, we used LysM-Cre mice which is important to note since LysM activity is present in cells within the myeloid lineage such as macrophages [25]. Several reports including our own [17] have shown that microglia are the only resident myeloid cells present in the spinal cord parenchyma in naïve states [19; 51], therefore the loss of TLR4 activity in LysM-TLR4$^{fl/fl}$ mice in the spinal cord is predominantly in microglia. It has been reported that LysM-Cre target only a subset of microglia (20–45% out of the total population [20; 61]), and it is noteworthy that targeting this subpopulation alone was sufficient to uncover the sex differences in our study.

Minocycline is frequently employed to reduce microglial activity and here we show that minocycline only attenuated pain-like behavior in male mice. In agreement with our work, i.t. administration of this drug attenuates both neuropathic and inflammatory pain-like behavior in male rodents [17; 24; 34; 36; 40; 55]. Furthermore, i.t. minocycline has been shown to be ineffective in reducing pain-like behavior in female rodents evoked by nerve injury [55], intra-plantar formalin injection [13] and antibody-induced arthritis [17], but was antinociceptive in bone cancer-induced pain model [66]. These studies employ different models, species or strains of rodents, doses of minocycline and timing of administration, which may account for different outcomes of minocycline treatment on pain-like behavior. A thorough investigation is thus needed to understand the inconsistencies of the antinociceptive effects of minocycline in females. Moreover, it is often oversimplified when relying on minocycline as a microglia inhibitor as this drug has well-documented anti-inflammatory properties that are not limited to microglia. Indeed, it is reducing microglial activity, but it is important to take into consideration that minocycline also can act on other cells, including T-cells, neutrophils, astrocytes and neurons [42]. Still, the fact that minocycline has sex-associated antinociceptive effects in some animal models of pain

testifies that there are differences between male and female pain mechanisms, and these should be further dissected.

As the sex-dependent effect of minocycline has been confirmed by several studies, we used in-depth proteomics with LC/MS-MS to further examine the downstream proteins regulating these sex differences. Our study highlights an interesting pattern that there is an upregulation of anti-inflammatory and antinociceptive proteins in male but not female mice that received minocycline. In particular, proteins of the serpin family, which are inhibitors of serine proteases, were well represented with levels of five serpin proteases, A1AT2, A1AT4, A1AT5, SAP3K and SAP3N, being significantly elevated in spinal cords from minocycline-treated male mice. On the contrary, we were surprised to find only few proteins being downregulated in response to minocycline. This could be a matter of such factors as i) being below detection limit, ii) being diluted during sample preparation as we here took a general approach rather than for example focus on membrane proteins, iii) being regulated by posttranslational modifications, and iv) having a lipid-based composition. In addition, changes in protein expression levels could arise as primary or secondary consequences of minocycline treatment and therefore our study does not delineate the cellular specificity of minocycline.

Targeting individual proteins that were upregulated following minocycline treatment produced none or modest antinociception. First, co-administration of haptoglobin with disulfide HMGB1 did not prevent pain-like behavior. As three out of five paralogs of alpha-1-antitrypsin were upregulated in the LC-MS/MS data we assessed the ability of alpha-1- antitrypsin to prevent and reverse i.t. disulfide HMGB1-induced hypersensitivity. Interestingly, alpha-1-antitrypsin partially reversed disulfide HMGB1-induced pain-like behavior in male but not female mice. Recent reports show that peripheral administration of alpha-1-antitrypsin is antinociceptive by preventing activation of neutrophil elastase and PAR2 [43; 44]. However, our results do not entirely support this linkage as we failed to demonstrate that inhibition of neutrophil elastase prevents disulfide HMGB1-induced hypersensitivity. In addition to neutrophil elastase, alpha-1-antitrypsin also blocks cathepsin G and proteinase 3 [39]. Hence, other proteases may be the link between alpha-1-antitrypsin and PAR2 activation, and the reason for why the antagonist sivelestat was not effective in alleviating hypersensitivity induced by disulfide HMGB1.

While spinal PAR2 has been implicated in several pain models [8; 14; 21; 26; 43; 44; 67], our study is the first to consider sex differences. Interestingly, PAR2 expression was downregulated in both sexes following minocycline treatment and PAR2 depletion ameliorated disulfide HMGB1-induced pain in both male and female mice. In the light of our hypothesis regarding the sex-dependent effect of minocycline this finding was rather unexpected. PAR2 is not only activated by neutrophil elastase, but also by trypsin and tryptase which have been detected in the CNS [16; 33]. Thus, it is possible that disulfide HMGB1 induce different signaling pathways in males and females which converge in PAR2 activation, and that minocycline only affects the linkage in male mice. Pinpointing the downstream signaling pathway that governs the sexual dimorphic effect of minocycline on HMGB1-induced pain appears to be complex. Therefore, further investigations of this as well as the other proteins identified by LC-MS/MS are warranted to gain a better

understanding of how these proteins interact and modulate the sex-dependent effects of minocycline.

In conclusion, even though disulfide HMGB1 induces pain-like behavior in both male and female mice, the mechanisms underlying its central pronociceptive effects on microglia are sex-dependent. Our findings support previous works showing that sexually dimorphic pain processing is present not only in humans but also in rodents, and highlights the importance of including animals of both sexes in order to optimize the translational potential of preclinical pain research. Our global protein approach uncovers an intriguing pattern suggesting differences in microglial function between males and females in which minocycline elevates factors associated with anti-inflammatory and antinociceptive properties in male mice only, but that there may be points of convergence. Several of the proteins identified as differentially regulated subsequent to minocycline administration represent exciting targets for future pain studies. Most certainly, a future challenge will be to decipher the exact mechanisms and molecular machinery that give minocycline its sex-specific actions.

Supplementary Material

Refer to Web version on PubMed Central for supplementary material.

Acknowledgements

This work was supported by Swedish Research Council (2013-8373 and 2015-02776), Ragnar Söderberg Foundation, Knut and Alice Wallenberg Foundation, William K. Bowes Foundation, Family Lundblad Foundation and the European Union Seventh Framework Programme (FP7/2007-2013) under grant agreement No. 602919 (GLORIA). R. Rudjito was funded by European Union Horizon 2020 research and innovation program under the Marie Sklodowska-Curie grant agreement No. 642720 (BonePain). K. Kultima was funded by ALF grants Region Uppsala, Strategic Funds Uppsala University Hospital and Magnus Bergvall Foundation. T.J. Price and M.D. Burton were funded by NIH grants NS098826 and NS096030 respectively. We also acknowledge Johan Lengqvist and Shibu Krishnan for technical assistance.

References

[1]. Abeyama K, Stern DM, Ito Y, Kawahara K, Yoshimoto Y, Tanaka M, Uchimura T, Ida N, Yamazaki Y, Yamada S, Yamamoto Y, Yamamoto H, Iino S, Taniguchi N, Maruyama I. The N-terminal domain of thrombomodulin sequesters high-mobility group-B1 protein, a novel antiinflammatory mechanism. The Journal of clinical investigation 2005;115(5):1267–1274. [PubMed: 15841214]

[2]. Agalave NM, Lane BT, Mody PH, Szabo-Pardi TA, Burton MD. Isolation, culture, and downstream characterization of primary microglia and astrocytes from adult rodent brain and spinal cord. Journal of neuroscience methods 2020;340:108742. [PubMed: 32315669]

[3]. Agalave NM, Larsson M, Abdelmoaty S, Su J, Baharpoor A, Lundback P, Palmblad K, Andersson U, Harris H, Svensson CI. Spinal HMGB1 induces TLR4-mediated long-lasting hypersensitivity and glial activation and regulates pain-like behavior in experimental arthritis. Pain 2014;155(9):1802–1813. [PubMed: 24954167]

[4]. Agalave NM, Svensson CI. Extracellular high-mobility group box 1 protein (HMGB1) as a mediator of persistent pain. Molecular medicine (Cambridge, Mass) 2015;20:569–578.

[5]. Allette YM, Due MR, Wilson SM, Feldman P, Ripsch MS, Khanna R, White FA. Identification of a functional interaction of HMGB1 with Receptor for Advanced Glycation End-products in a model of neuropathic pain. Brain Behav Immun 2014;42:169–177. [PubMed: 25014009]

[6]. Aucott H, Sowinska A, Harris HE, Lundback P. Ligation of free HMGB1 to TLR2 in the absence of ligand is negatively regulated by the C-terminal tail domain. Molecular medicine (Cambridge, Mass) 2018;24(1):19.

[7]. Ballman KV, Grill DE, Oberg AL, Therneau TM. Faster cyclic loess: normalizing RNA arrays via linear models. Bioinformatics 2004;20(16):2778–2786. [PubMed: 15166021]

[8]. Bao Y, Hou W, Liu R, Gao Y, Kong X, Yang L, Shi Z, Li W, Zheng H, Jiang S, Li C, Qin Y, Hua B. PAR2-mediated upregulation of BDNF contributes to central sensitization in bone cancer pain. Molecular pain 2014;10:28. [PubMed: 24886294]

[9]. Barbour KW, Wei F, Brannan C, Flotte TR, Baumann H, Berger FG. The murine alpha(1)-proteinase inhibitor gene family: polymorphism, chromosomal location, and structure. Genomics 2002;80(5):515–522. [PubMed: 12408969]

[10]. Beggs S, Salter MW. The known knowns of microglia-neuronal signalling in neuropathic pain. Neuroscience letters 2013;557 Pt A:37–42. [PubMed: 23994389]

[11]. Boyle DL, Rosengren S, Bugbee W, Kavanaugh A, Firestein GS. Quantitative biomarker analysis of synovial gene expression by real-time PCR. Arthritis Res Ther 2003;5(6):R352–360. [PubMed: 14680510]

[12]. Chaplan SR, Bach FW, Pogrel JW, Chung JM, Yaksh TL. Quantitative assessment of tactile allodynia in the rat paw. Journal of neuroscience methods 1994;53(1):55–63. [PubMed: 7990513]

[13]. Chen G, Luo X, Qadri MY, Berta T, Ji RR. Sex-Dependent Glial Signaling in Pathological Pain: Distinct Roles of Spinal Microglia and Astrocytes. Neurosci Bull 2017.

[14]. Chen K, Zhang ZF, Liao MF, Yao WL, Wang J, Wang XR. Blocking PAR2 attenuates oxaliplatin-induced neuropathic pain via TRPV1 and releases of substance P and CGRP in superficial dorsal horn of spinal cord. Journal of the neurological sciences 2015;352(1–2):62–67. [PubMed: 25829079]

[15]. Das N, Dewan V, Grace PM, Gunn RJ, Tamura R, Tzarum N, Watkins LR, Wilson IA, Yin H. HMGB1 Activates Proinflammatory Signaling via TLR5 Leading to Allodynia. Cell Rep 2016;17(4):1128–1140. [PubMed: 27760316]

[16]. Dong H, Wang Y, Zhang X, Zhang X, Qian Y, Ding H, Zhang S. Stabilization of Brain Mast Cells Alleviates LPS-Induced Neuroinflammation by Inhibiting Microglia Activation. Frontiers in cellular neuroscience 2019;13:191. [PubMed: 31130850]

[17]. Fernandez-Zafra T, Gao T, Jurczak A, Sandor K, Hore Z, Agalave NM, Su J, Estelius J, Lampa J, Hokfelt T, Wiesenfeld-Hallin Z, Xu X, Denk F, Svensson CI. Exploring the transcriptome of resident spinal microglia after collagen antibody-induced arthritis. Pain 2018.

[18]. Gao HM, Zhou H, Zhang F, Wilson BC, Kam W, Hong JS. HMGB1 acts on microglia Mac1 to mediate chronic neuroinflammation that drives progressive neurodegeneration. J Neurosci 2011;31(3):1081–1092. [PubMed: 21248133]

[19]. Goldmann T, Wieghofer P, Jordao MJ, Prutek F, Hagemeyer N, Frenzel K, Amann L, Staszewski O, Kierdorf K, Krueger M, Locatelli G, Hochgerner H, Zeiser R, Epelman S, Geissmann F, Priller J, Rossi FM, Bechmann I, Kerschensteiner M, Linnarsson S, Jung S, Prinz M. Origin, fate and dynamics of macrophages at central nervous system interfaces. Nature immunology 2016;17(7):797–805. [PubMed: 27135602]

[20]. Goldmann T, Wieghofer P, Muller PF, Wolf Y, Varol D, Yona S, Brendecke SM, Kierdorf K, Staszewski O, Datta M, Luedde T, Heikenwalder M, Jung S, Prinz M. A new type of microglia gene targeting shows TAK1 to be pivotal in CNS autoimmune inflammation. Nature neuroscience 2013;16(11):1618–1626. [PubMed: 24077561]

[21]. Hassler SN, Ahmad FB, Burgos-Vega CC, Boitano S, Vagner J, Price TJ, Dussor G. Protease activated receptor 2 (PAR2) activation causes migraine-like pain behaviors in mice. Cephalalgia : an international journal of headache 2019;39(1):111–122. [PubMed: 29848111]

[22]. Hassler SN, Kume M, Mwirigi JM, Ahmad A, Shiers S, Wangzhou A, Ray PR, Belugin SN, Naik DK, Burton MD, Vagner J, Boitano S, Akopian AN, Dussor G, Price TJ.

[23]. Hayakawa K, Arai K, Lo EH. Role of ERK map kinase and CRM1 in IL-1beta-stimulated release of HMGB1 from cortical astrocytes. Glia 2010;58(8):1007–1015. [PubMed: 20222144]

[24]. Hua XY, Svensson CI, Matsui T, Fitzsimmons B, Yaksh TL, Webb M. Intrathecal minocycline attenuates peripheral inflammation-induced hyperalgesia by inhibiting p38 MAPK in spinal microglia. Eur J Neurosci 2005;22(10):2431–2440. [PubMed: 16307586]

[25]. Jia L, Vianna CR, Fukuda M, Berglund ED, Liu C, Tao C, Sun K, Liu T, Harper MJ, Lee CE, Lee S, Scherer PE, Elmquist JK. Hepatocyte Toll-like receptor 4 regulates obesity-induced inflammation and insulin resistance. Nat Commun 2014;5:3878. [PubMed: 24815961]

[26]. Jimenez-Vargas NN, Pattison LA, Zhao P, Lieu T, Latorre R, Jensen DD, Castro J, Aurelio L, Le GT, Flynn B, Herenbrink CK, Yeatman HR, Edgington-Mitchell L, Porter CJH, Halls ML, Canals M, Veldhuis NA, Poole DP, McLean P, Hicks GA, Scheff N, Chen E, Bhattacharya A, Schmidt BL, Brierley SM, Vanner SJ, Bunnett NW. Protease-activated receptor-2 in endosomes signals persistent pain of irritable bowel syndrome. Proceedings of the National Academy of Sciences of the United States of America 2018;115(31):E7438–e7447. [PubMed: 30012612]

[27]. Kall L, Canterbury JD, Weston J, Noble WS, MacCoss MJ. Semi-supervised learning for peptide identification from shotgun proteomics datasets. Nat Methods 2007;4(11):923–925. [PubMed: 17952086]

[28]. Kall L, Storey JD, MacCoss MJ, Noble WS. Posterior error probabilities and false discovery rates: two sides of the same coin. Journal of proteome research 2008;7(1):40–44. [PubMed: 18052118]

[29]. Kawabata K, Suzuki M, Sugitani M, Imaki K, Toda M, Miyamoto T. ONO-5046, a novel inhibitor of human neutrophil elastase. Biochemical and biophysical research communications 1991;177(2):814–820. [PubMed: 2049103]

[30]. Kessner D, Chambers M, Burke R, Agus D, Mallick P. ProteoWizard: open source software for rapid proteomics tools development. Bioinformatics 2008;24(21):2534–2536. [PubMed: 18606607]

[31]. Kim S, Pevzner PA. MS-GF+ makes progress towards a universal database search tool for proteomics. Nat Commun 2014;5:5277. [PubMed: 25358478]

[32]. Kokkola R, Andersson A, Mullins G, Ostberg T, Treutiger CJ, Arnold B, Nawroth P, Andersson U, Harris RA, Harris HE. RAGE is the major receptor for the proinflammatory activity of HMGB1 in rodent macrophages. Scandinavian journal of immunology 2005;61(1):1–9. [PubMed: 15644117]

[33]. Koshikawa N, Hasegawa S, Nagashima Y, Mitsuhashi K, Tsubota Y, Miyata S, Miyagi Y, Yasumitsu H, Miyazaki K. Expression of trypsin by epithelial cells of various tissues, leukocytes, and neurons in human and mouse. The American journal of pathology 1998;153(3):937–944. [PubMed: 9736042]

[34]. Ledeboer A, Sloane EM, Milligan ED, Frank MG, Mahony JH, Maier SF, Watkins LR. Minocycline attenuates mechanical allodynia and proinflammatory cytokine expression in rat models of pain facilitation. Pain 2005;115(1–2):71–83. [PubMed: 15836971]

[35]. Lehnardt S, Massillon L, Follett P, Jensen FE, Ratan R, Rosenberg PA, Volpe JJ, Vartanian T. Activation of innate immunity in the CNS triggers neurodegeneration through a Toll-like receptor 4-dependent pathway. Proceedings of the National Academy of Sciences of the United States of America 2003;100(14):8514–8519. [PubMed: 12824464]

[36]. Lin CS, Tsaur ML, Chen CC, Wang TY, Lin CF, Lai YL, Hsu TC, Pan YY, Yang CH, Cheng JK. Chronic intrathecal infusion of minocycline prevents the development of spinal-nerve ligation-induced pain in rats. Reg Anesth Pain Med 2007;32(3):209–216. [PubMed: 17543815]

[37]. Loram LC, Sholar PW, Taylor FR, Wiesler JL, Babb JA, Strand KA, Berkelhammer D, Day HE, Maier SF, Watkins LR. Sex and estradiol influence glial pro-inflammatory responses to lipopolysaccharide in rats. Psychoneuroendocrinology 2012;37(10):1688–1699. [PubMed: 22497984]

[38]. McMahon SB, Malcangio M. Current challenges in glia-pain biology. Neuron 2009;64(1):46–54. [PubMed: 19840548]

[39]. Mihara K, Ramachandran R, Renaux B, Saifeddine M, Hollenberg MD. Neutrophil elastase and proteinase-3 trigger G protein-biased signaling through proteinase-activated receptor-1 (PAR1). The Journal of biological chemistry 2013;288(46):32979–32990. [PubMed: 24052258]

[40]. Mika J, Zychowska M, Popiolek-Barczyk K, Rojewska E, Przewlocka B. Importance of glial activation in neuropathic pain. European journal of pharmacology 2013;716(1–3):106–119. [PubMed: 23500198]

[41]. Milligan ED, Watkins LR. Pathological and protective roles of glia in chronic pain. Nature reviews Neuroscience 2009;10(1):23–36. [PubMed: 19096368]

[42]. Moller T, Bard F, Bhattacharya A, Biber K, Campbell B, Dale E, Eder C, Gan L, Garden GA, Hughes ZA, Pearse DD, Staal RG, Sayed FA, Wes PD, Boddeke HW. Critical data-based re-evaluation of minocycline as a putative specific microglia inhibitor. Glia 2016;64(10):1788–1794. [PubMed: 27246804]

[43]. Muley MM, Krustev E, Reid AR, McDougall JJ. Prophylactic inhibition of neutrophil elastase prevents the development of chronic neuropathic pain in osteoarthritic mice. Journal of neuroinflammation 2017;14(1):168. [PubMed: 28835277]

[44]. Muley MM, Reid AR, Botz B, Bolcskei K, Helyes Z, McDougall JJ. Neutrophil elastase induces inflammation and pain in mouse knee joints via activation of proteinase-activated receptor-2. British journal of pharmacology 2016;173(4):766–777. [PubMed: 26140667]

[45]. O'Connor KA, Hansen MK, Rachal Pugh C, Deak MM, Biedenkapp JC, Milligan ED, Johnson JD, Wang H, Maier SF, Tracey KJ, Watkins LR. Further characterization of high mobility group box 1 (HMGB1) as a proinflammatory cytokine: central nervous system effects. Cytokine 2003;24(6):254–265. [PubMed: 14609567]

[46]. Ritchie ME, Phipson B, Wu D, Hu Y, Law CW, Shi W, Smyth GK. limma powers differential expression analyses for RNA-sequencing and microarray studies. Nucleic Acids Res 2015;43(7):e47. [PubMed: 25605792]

[47]. Romero-Sandoval A, Chai N, Nutile-McMenemy N, Deleo JA. A comparison of spinal Iba1 and GFAP expression in rodent models of acute and chronic pain. Brain research 2008;1219:116–126. [PubMed: 18538310]

[48]. Rost HL, Sachsenberg T, Aiche S, Bielow C, Weisser H, Aicheler F, Andreotti S, Ehrlich HC, Gutenbrunner P, Kenar E, Liang X, Nahnsen S, Nilse L, Pfeuffer J, Rosenberger G, Rurik M, Schmitt U, Veit J, Walzer M, Wojnar D, Wolski WE, Schilling O, Choudhary JS, Malmstrom L, Aebersold R, Reinert K, Kohlbacher O. OpenMS: a flexible open-source software platform for mass spectrometry data analysis. Nat Methods 2016;13(9):741–748. [PubMed: 27575624]

[49]. Sekiguchi F, Domoto R, Nakashima K, Yamasoba D, Yamanishi H, Tsubota M, Wake H, Nishibori M, Kawabata A. Paclitaxel-induced HMGB1 release from macrophages and its implication for peripheral neuropathy in mice: Evidence for a neuroimmune crosstalk. Neuropharmacology 2018;141:201–213. [PubMed: 30179591]

[50]. Serang O, MacCoss MJ, Noble WS. Efficient marginalization to compute protein posterior probabilities from shotgun mass spectrometry data. Journal of proteome research 2010;9(10):5346–5357. [PubMed: 20712337]

[51]. Shemer A, Erny D, Jung S, Prinz M. Microglia Plasticity During Health and Disease: An Immunological Perspective. Trends in immunology 2015;36(10):614–624. [PubMed: 26431939]

[52]. Shi Y, Zhang L, Teng J, Miao W. HMGB1 mediates microglia activation via the TLR4/NF-kappaB pathway in coriaria lactone induced epilepsy. Molecular medicine reports 2018;17(4):5125–5131. [PubMed: 29393419]

[53]. Sierra A, Gottfried-Blackmore AC, McEwen BS, Bulloch K. Microglia derived from aging mice exhibit an altered inflammatory profile. Glia 2007;55(4):412–424. [PubMed: 17203473]

[54]. Sorge RE, LaCroix-Fralish ML, Tuttle AH, Sotocinal SG, Austin JS, Ritchie J, Chanda ML, Graham AC, Topham L, Beggs S, Salter MW, Mogil JS. Spinal cord Toll-like receptor 4 mediates inflammatory and neuropathic hypersensitivity in male but not female mice. J Neurosci 2011;31(43):15450–15454. [PubMed: 22031891]

[55]. Sorge RE, Mapplebeck JC, Rosen S, Beggs S, Taves S, Alexander JK, Martin LJ, Austin JS, Sotocinal SG, Chen D, Yang M, Shi XQ, Huang H, Pillon NJ, Bilan PJ, Tu Y, Klip A, Ji RR, Zhang J, Salter MW, Mogil JS. Different immune cells mediate mechanical pain hypersensitivity in male and female mice. Nature neuroscience 2015;18(8):1081–1083. [PubMed: 26120961]

[56]. Taves S, Berta T, Liu DL, Gan S, Chen G, Kim YH, Van de Ven T, Laufer S, Ji RR. Spinal inhibition of p38 MAP kinase reduces inflammatory and neuropathic pain in male but not female

mice: Sex-dependent microglial signaling in the spinal cord. Brain Behav Immun 2016;55:70–81. [PubMed: 26472019]

[57]. Tsuda M, Beggs S, Salter MW, Inoue K. Microglia and intractable chronic pain. Glia 2013;61(1):55–61. [PubMed: 22740331]

[58]. Tsuda M, Inoue K, Salter MW. Neuropathic pain and spinal microglia: a big problem from molecules in “small” glia. Trends Neurosci 2005;28(2):101–107. [PubMed: 15667933]

[59]. Venereau E, Casalgrandi M, Schiraldi M, Antoine DJ, Cattaneo A, De Marchis F, Liu J, Antonelli A, Preti A, Raeli L, Shams SS, Yang H, Varani L, Andersson U, Tracey KJ, Bachi A, Uguccioni M, Bianchi ME. Mutually exclusive redox forms of HMGB1 promote cell recruitment or proinflammatory cytokine release. The Journal of experimental medicine 2012;209(9):1519–1528. [PubMed: 22869893]

[60]. Vicuna L, Strochlic DE, Latremoliere A, Bali KK, Simonetti M, Husainie D, Prokosch S, Riva P, Griffin RS, Njoo C, Gehrig S, Mall MA, Arnold B, Devor M, Woolf CJ, Liberles SD, Costigan M, Kuner R. The serine protease inhibitor SerpinA3N attenuates neuropathic pain by inhibiting T cell-derived leukocyte elastase. Nature medicine 2015;21(5):518–523.

[61]. Wang J, Wegener JE, Huang TW, Sripathy S, De Jesus-Cortes H, Xu P, Tran S, Knobbe W, Leko V, Britt J, Starwalt R, McDaniel L, Ward CS, Parra D, Newcomb B, Lao U, Nourigat C, Flowers DA, Cullen S, Jorstad NL, Yang Y, Glaskova L, Vingeau S, Kozlitina J, Yetman MJ, Jankowsky JL, Reichardt SD, Reichardt HM, Gartner J, Bartolomei MS, Fang M, Loeb K, Keene CD, Bernstein I, Goodell M, Brat DJ, Huppke P, Neul JL, Bedalov A, Pieper AA. Wild-type microglia do not reverse pathology in mouse models of Rett syndrome. Nature 2015;521(7552):E1–4. [PubMed: 25993969]

[62]. Woller SA, Ravula SB, Tucci FC, Beaton G, Corr M, Isseroff RR, Soulika AM, Chigbrow M, Eddinger KA, Yaksh TL. Systemic TAK-242 prevents intrathecal LPS evoked hyperalgesia in male, but not female mice and prevents delayed allodynia following intraplantar formalin in both male and female mice: The role of TLR4 in the evolution of a persistent pain state. Brain Behav Immun 2016;56:271–280. [PubMed: 27044335]

[63]. Yanai H, Matsuda A, An J, Koshiba R, Nishio J, Negishi H, Ikushima H, Onoe T, Ohdan H, Yoshida N, Taniguchi T. Conditional ablation of HMGB1 in mice reveals its protective function against endotoxemia and bacterial infection. Proceedings of the National Academy of Sciences of the United States of America 2013;110(51):20699–20704. [PubMed: 24302768]

[64]. Yang H, Lundback P, Ottosson L, Erlandsson-Harris H, Venereau E, Bianchi ME, Al-Abed Y, Andersson U, Tracey KJ, Antoine DJ. Redox modification of cysteine residues regulates the cytokine activity of high mobility group box-1 (HMGB1). Molecular medicine (Cambridge, Mass) 2012;18:250–259.

[65]. Yang H, Wang H, Levine YA, Gunasekaran MK, Wang Y, Addorisio M, Zhu S, Li W, Li J, de Kleijn DP, Olofsson PS, Warren HS, He M, Al-Abed Y, Roth J, Antoine DJ, Chavan SS, Andersson U, Tracey KJ. Identification of CD163 as an antiinflammatory receptor for HMGB1-haptoglobin complexes. JCI insight 2016;1(7).

[66]. Yang Y, Li H, Li TT, Luo H, Gu XY, Lu N, Ji RR, Zhang YQ. Delayed activation of spinal microglia contributes to the maintenance of bone cancer pain in female Wistar rats via P2X7 receptor and IL-18. J Neurosci 2015;35(20):7950–7963. [PubMed: 25995479]

[67]. Zhao P, Lieu T, Barlow N, Sostegni S, Haerteis S, Korbmacher C, Liedtke W, Jimenez-Vargas NN, Vanner SJ, Bunnett NW. Neutrophil Elastase Activates Protease-activated Receptor-2 (PAR2) and Transient Receptor Potential Vanilloid 4 (TRPV4) to Cause Inflammation and Pain. The Journal of biological chemistry 2015;290(22):13875–13887. [PubMed: 25878251]

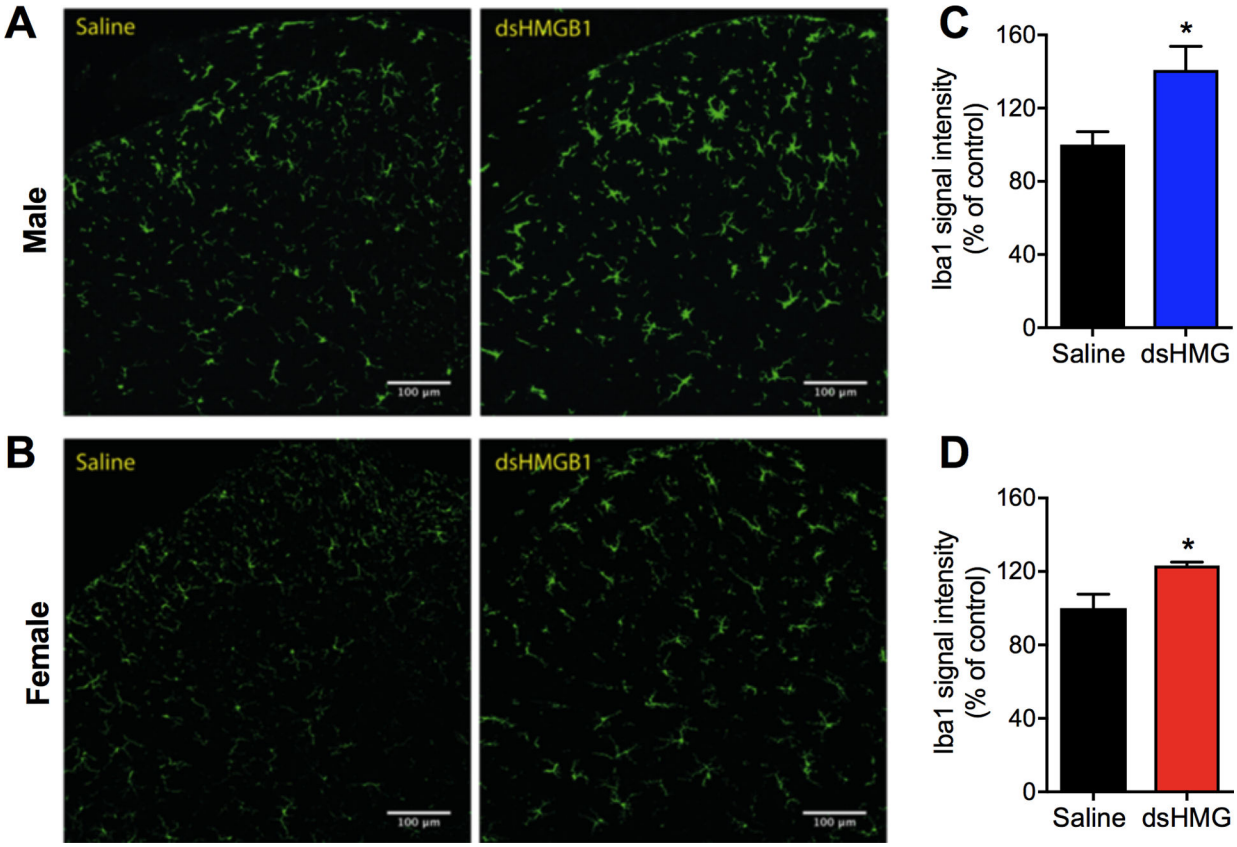

Figure 1. Intrathecal injection of disulfide HMGB1 leads to upregulation of Iba1 expression in spinal lumbar dorsal horn.

Representative confocal images of Iba1 immunoreactivity in (A) male and (B) female spinal dorsal horns 24 h postinjection of either vehicle (saline) or disulfide HMGB1. Bar graphs display quantification of Iba1 signal intensity in (C) male and (D) female mice expressed as percentage change to the control saline group. Data are presented as the mean ± SEM, n=5–6 mice/group. *p<0.05 vs. control group. dsHMG: disulfide HMGB1, scale bar: 100 μm.

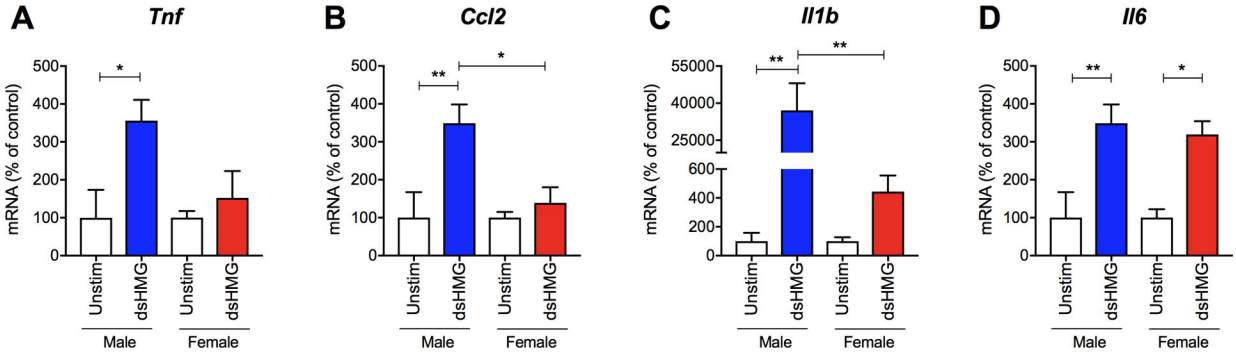

Figure 2. Disulfide HMGB1 induces cytokine and chemokine expression to higher levels in primary microglial culture generated from male compared to female mice.

Bar graphs represent mRNA levels for A) *Tnf*, B) *Ccl2*, C) *Il1b* and D) *Il6* in primary cultures of microglia 6 h following stimulation with disulfide HMGB1 (1 μg/ml) or no stimulation. Data are represented as mean ± SEM, n=4–5 experimental replicates/group, *p<0.05, **p<0.01 vs. unstimulated group. Unstim: unstimulated, dsHMG: disulfide HMGB1.

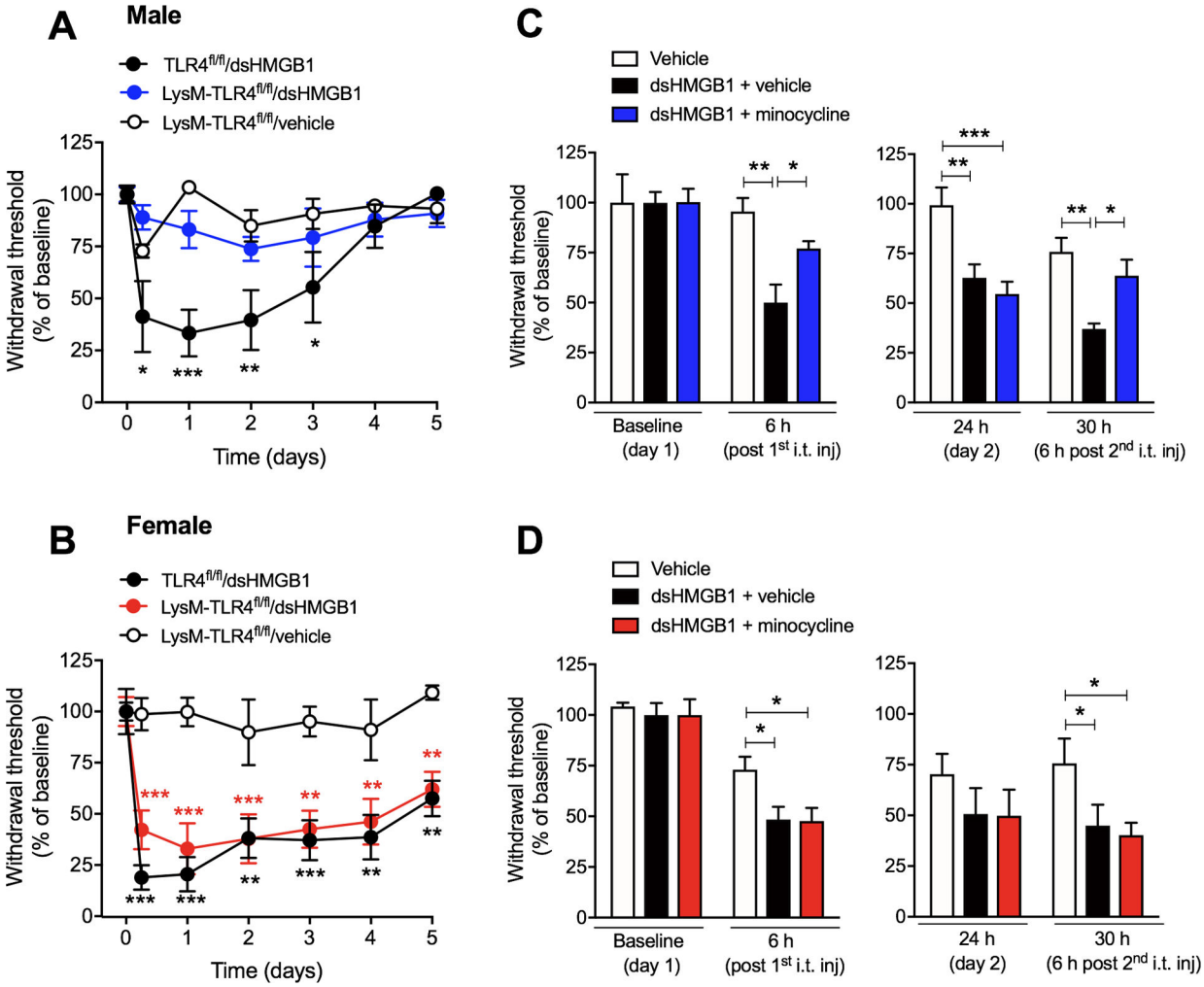

Figure 3. Blockade of microglial function elicits antinociceptive effects in disulfide HMGB1-subjected male but not female mice.

Withdrawal threshold values after i.t. injection of dsHMGB1 (1 μg/mouse) or vehicle (saline) in (A) male and (B) female mice lacking TLR4 in microglia (LysM-TLR4$^{fl/fl}$) or TLR4$^{fl/fl}$ (control mice). Withdrawal response prior to, 6 h and 24 h after the first day i.t. injection of a combination of disulfide HMGB1 (1 μg/mouse) and minocycline (30 μg/mouse, microglial inhibitor) or disulfide HMGB1 (1 μg/mouse) and vehicle (PBS), as well as 6 h after the second day intrathecal injection of minocycline (30 μg/mouse) or vehicle in (C) male and (D) female mice. Data are presented as mean ± SEM, n=4–8 mice/group, *p<0.05, **p<0.01, ***p<0.001 vs. vehicle groups.

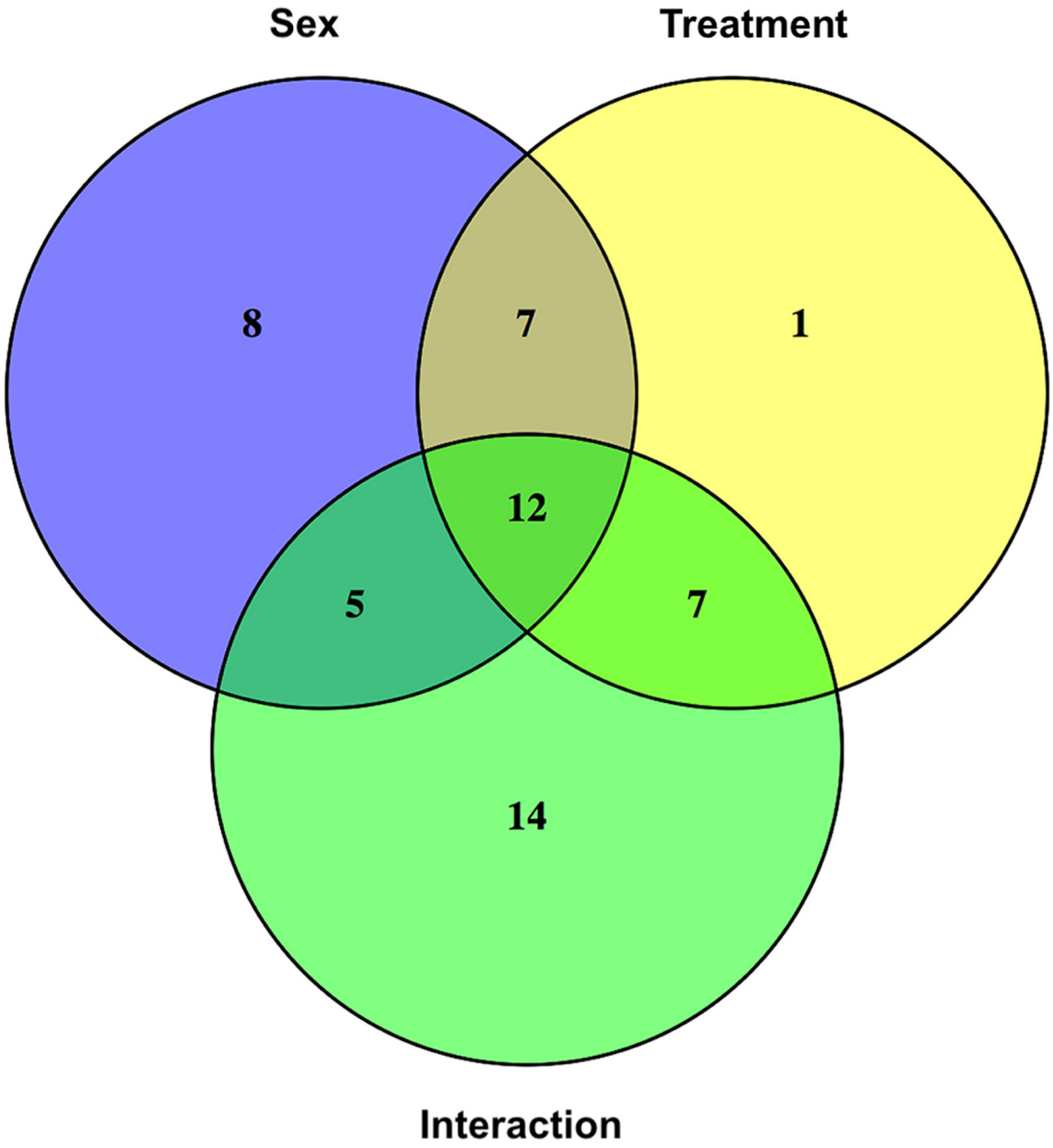

Figure 4. LC/MS-MS reveals 12 spinal proteins to be differentially expressed in response to sex and minocycline treatment.

Venn diagram displays three statistically significant contrasts ($p<0.05$) - sex difference, treatment effect and the interaction between sex and treatment - analyzed in the 54 proteins identified by LC-MS/MS.

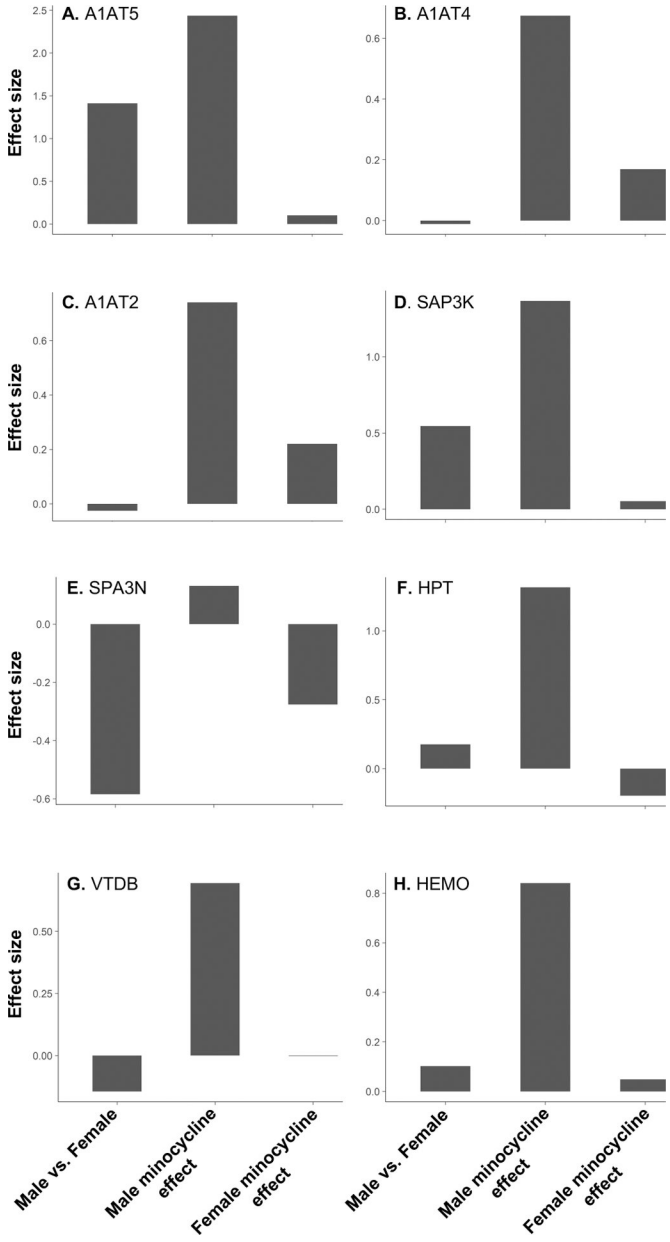

Figure 5. Minocycline treatment induces upregulation of antiinflammatory and antinociceptive factors in the spinal dorsal horns of disulfide HMGB1-subjected male but not female mice.

Bar graphs depict the effect size in protein expression of (A) A1AT5, (B) A1AT4, (C) A1AT2, (D) SAP3K, (E) SAP3N, (F) HPT, (G) VTDB and (H) HEMO between i) male vs. female injected with disulfide HMGB1, ii) males injected with disulfide HMGB1-minocycline compared to disulfide HMGB1-vehicle and iii) females injected with disulfide HMGB1-minocyline compared to disulfide HMGB1-vehicle. Data are presented as relative levels in $\log_2$ scale, n=6 mice/group.

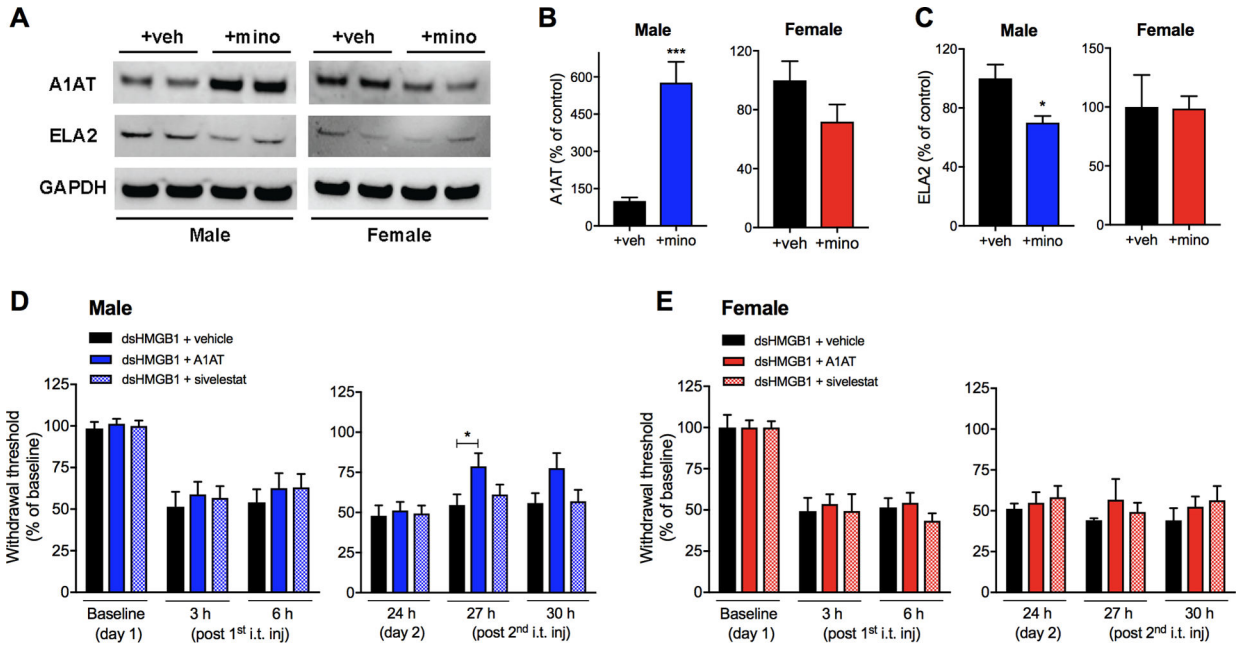

Figure 6. Alpha-1-antitrypsin, but not its downstream target neutrophil elastase, partially reverses disulfide HMGB1-induced pain-like behavior in male but not female mice.

Representative western blot images of (A) alpha-1-antitrypsin (A1AT), neutrophil elastase (ELA2) and GAPDH from protein extracts of lumbar spinal cords of male and female mice injected with disulfide HMGB1 in combination with vehicle (+veh) or minocycline (+mino). Bar graphs depict quantification of (B) A1AT and (C) ELA2 immunopositive bands normalized to GAPDH and presented as percentage change to vehicle control groups. Withdrawal response prior to, 3 h, 6 h and 24 h after the first day i.t. injection of disulfide HMGB1 (1 μg/mouse) in combination with either alpha-1-antitrypsin (15 ng/mouse), sivelestat (0.5 ng, neutrophil elastase inhibitor) or vehicle (PBS), and 3 and 6 h after the second day i.t. injection of either alpha-1-antitrypsin (30 ng/mouse), sivelestat (1 ng/mouse) or vehicle in (D) male and (E) female mice. Data are presented as mean ± SEM, n=6 mice/group for western blot results and n=5–12 mice/group for behavioral results, *p<0.05, ***p<0.001 vs. control groups.

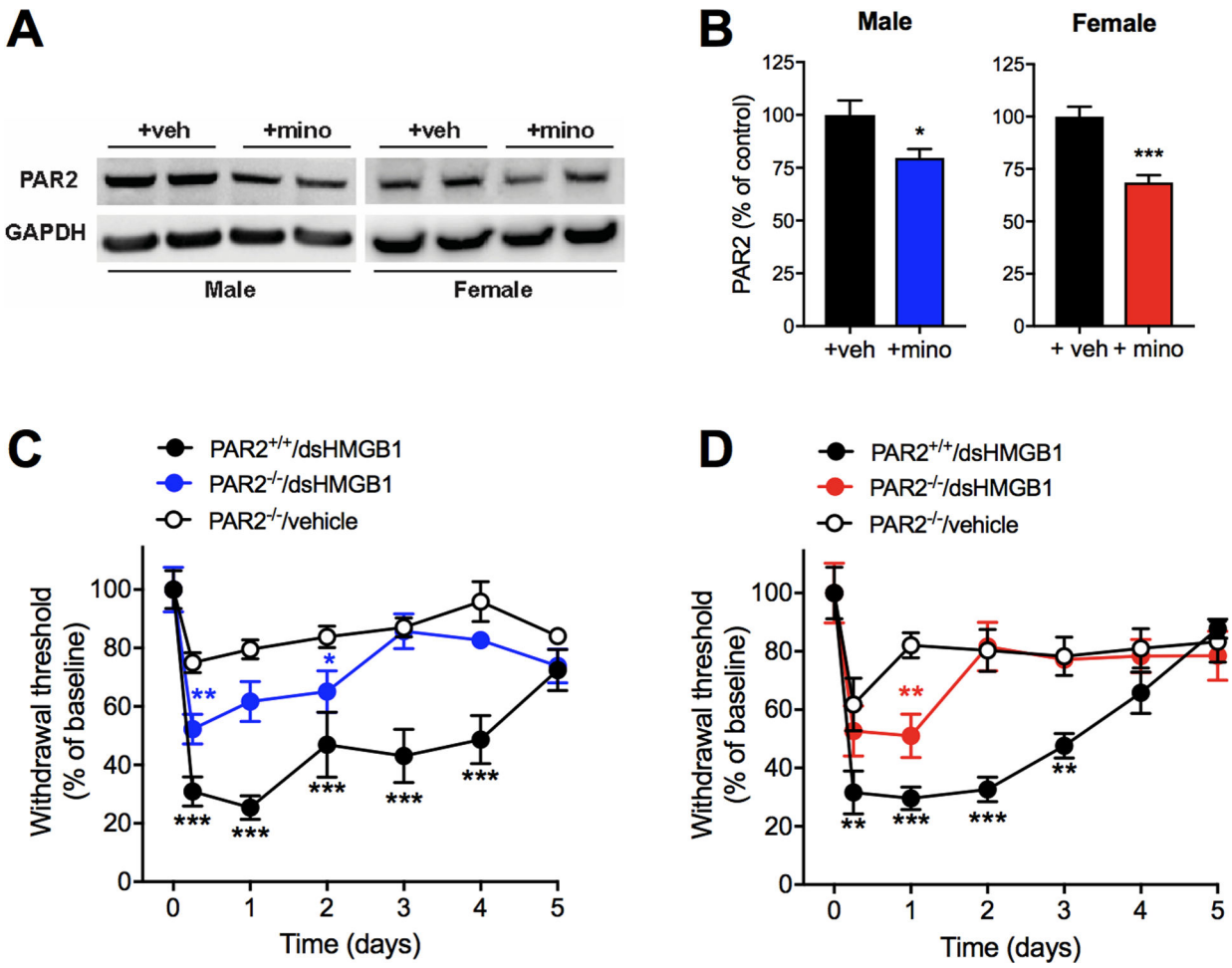

Figure 7. PAR2 depletion partially protects male and female mice from developing disulfide HMGB1-induced mechanical hypersensitivity.

(A) Representative western blot images and (B) quantification of proteinase-activated receptor 2 (PAR2) immunopositive bands normalized to GAPDH and presented as percentage change to vehicle control groups. Withdrawal response following i.t. injection of dsHMGB1 (1 μg) or vehicle in (C) male and (D) female wild-type ($PAR2^{+/+}$) and whole-body PAR2 knockout ($PAR2^{-/-}$) mice. Data are presented as mean ± SEM, n=6 mice/group for western blot results and n=4–7 mice/group for behavioral results, *p<0.05, **p<0.01, ***p<0.001 vs. control groups.